Supercritical Carbon Dioxide Turbine Design and Arrangement Optimization

Zhenya Li, Wenjie Bian, Li Jiang, Chuanliang Liu *, Jinyuan Shi and Ning Hao

Shanghai Power Equipment Research Institute Co. Ltd, Shanghai, China

To achieve a supercritical CO_2 cycle power generation system, a 25 MW supercritical CO_2 turbine rotor and cylinder were designed. Then, two compact arrangement schemes were proposed in this paper for the optimization of a supercritical CO_2 turbine rotor. In Scheme 1, the balance piston was arranged in the cooling gas section, which was more conducive to the arrangement of the dry gas seal. In Scheme II, the oil bearing was replaced by the gas bearing, and the dry gas seals at both ends of the turbine were installed outside the gas bearing, which was combined with the cooling gas section. The results suggest that the length of the rotor is reduced by 9% and 17% based on the above two schemes. The compact arrangement of the supercritical CO_2 turbine can well reduce the shaft length of the turbine, which is beneficial to the structural design and operation of the supercritical CO_2 turbine.

Keywords: supercritical carbon dioxide, turbomachinery, rotor design, compact arrangement, arrangement optimization

1 INTRODUCTION

Carbon dioxide has been widely used in supercritical carbon dioxide (sCO_2) Brayton cycle and transcritical carbon dioxide refrigeration cycle as working fluid (Yu et al., 2020). The combined system coupling sCO_2 Brayton cycle and refrigeration cycle could simultaneously produce power and cooling, exhibits great potential in green buildings, waste heat recovery, and industrial power supply (Wu C. et al., 2020; Khanmohammadi et al., 2020; Du et al., 2022). The sCO_2 cycle power generation system has high efficiency in a certain temperature range (Crespi et al., 2017; Li et al., 2020) and has advantages such as a small size, compact structure and so on (Ahn et al., 2015; Liao et al., 2019; Wu P. et al., 2020). It is a novel power generation technology that is currently a crucial research topic worldwide. It has broad application prospects in solar thermal power generation, small nuclear power, industrial waste heat and ship power (Qi et al., 2018; Mohammed et al., 2020; Guo et al., 2022).

Turbines are one of the core components of the sCO_2 power generation cycle. Due to its requests of high temperature, high pressure, high speed, and frequent start-and-stop, the design of turbine structures has become an important research field for scientific researchers and designers (Crespi et al., 2017; Luo et al., 2017). The rotor is the key component of the sCO_2 turbine unit. A reasonable arrangement of the rotor structure affects the overall shaft length and the design of the inner and outer cylinder structure, which is extremely important for the safety and reliability of the turbine. To ensure the efficient and smooth operation of the turbine, it is crucial for designers to study the reasonable arrangement of the sCO_2 turbine rotor.

For many years, researchers in various countries have performed much research on sCO_2 turbines and obtained many research results. For example, some institutes, such as Sandia Laboratories in the United States, Tokyo Institute of Technology in Japan, and the Korea Advanced Institute of Science and Technology, have designed the rotor of sCO_2 turbines and have put them into operation in the

laboratory. Odabaee et al.(Odabaee et al., 2016) used a 100 kW sCO_2 radial turbine with an inlet temperature of 560°C as the research focus and carried out an aerodynamic design on the turbine. In this study, the physical property data obtained by numerical calculation were compared with the NIST database, but the results showed that it was difficult to obtain accurate physical property data by fitting the gas state equation. In addition, Lee et al. considered the effects of the nonlinear physical property variation of the sCO_2 near the critical point in the traditional design method (Lee et al., 2012). The selection of an sCO_2 turbine was proposed by comparing important parameters such as the power and efficiency of sCO_2 turbines. In addition, Kim et al. conducted aerodynamic analysis on the sCO_2 turbine designed by the Korea Advanced Institute of Science and Technology and optimized the blades to improve the aerodynamic efficiency of the turbine (Kim et al., 2006; Kim et al., 2008). Schmitt et al. designed a 6-stage sCO_2 turbine with a power of 100 MW and an inlet temperature of 1,077°C (Schmitt et al., 2014). In this study, the parameters of the speed triangle were optimized, and the total power and efficiency of the turbine met the design requirements. Marion et al. developed a sCO_2 turbine applied to sCO_2-based power cycling to realize concentrated solar energy conversion in the SunShot project (Marion et al., 2019). In addition, Kalra et al. also jointly designed a 16 MW sCO_2 turbine conceptual diagram in the STEP (Supercritical Transformational Electric Power) project (Kalra et al., 2014). It indicated that the aerodynamic performance was improved by shearing rings instead of bolts. Feng et al. carried out aerodynamic analysis on 15 MW axial-flow sCO_2 turbines and 1.5 MW radial turbines based on the design of two different structural forms of sCO_2 turbines (Zhang et al., 2015). Xie et al. determined the shape of the nozzle and impeller by thermal design and linear design of a 200 kW sCO_2 radial turbine (Shi et al., 2015). They found that increasing the inlet height of the turbine impeller can reduce the manufacturing difficulty and the loss of secondary flow. The team also proposed a sCO_2 turbine that can adapt to a wide range of pressures and flow rates (Wang et al., 2016). The results show that the designed turbine can adaptively adjust the installation angle of the nozzle to correspond to different flow areas and adapt to different flow conditions.

Based on the above studies, it found that foreign countries have not only conducted in-depth research on the physical properties of sCO_2 and the aerodynamic design of turbines but have also made great progress in the overall layout and structural design of turbines. However, domestic research is still limited to sCO_2 aerodynamic design and flow arrangement. There are few studies on the compact overall arrangement of turbine rotors. Therefore, it is of great significance to improve the in-depth study of the compact arrangement of sCO_2 turbine rotors. With the purpose of creating a sCO_2 cycle power generation system, a 25 MW sCO_2 turbine rotor and cylinder were designed in this paper. Then, two compact arrangement schemes were proposed for the optimization of the sCO_2 turbine rotor in this paper. Finally, the advantages of the compact arrangement were analyzed by comparison with the traditional scheme.
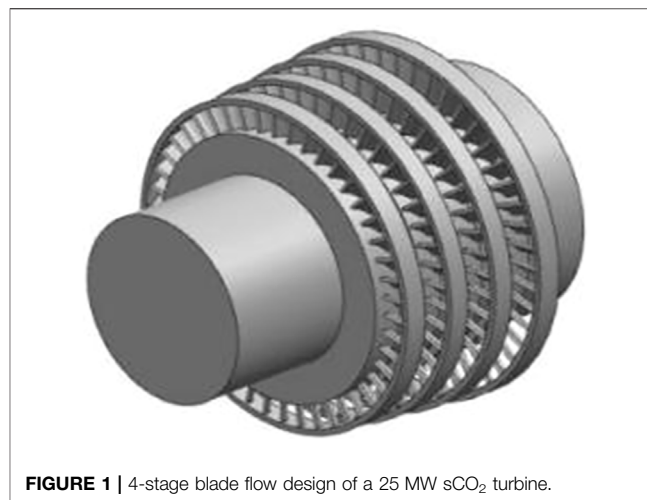

FIGURE 1 | 4-stage blade flow design of a 25 MW sCO_2 turbine.

TABLE 1 | Basic properties of CO_2.

Physical Property	Value
Molar mass M/kg·kmol^{-1}	44.01
Critical temperature T_c/K	304.21
Critical pressure P_c/MPa	7.38
Critical density ρ/kg·m^{-3}	383.98

TABLE 2 | Design parameters.

Design Parameters	Value
Inlet pressure P_0/MPa	24
Inlet temperature T_0/K	873
Outlet pressure P_2/MPa	8.5
Mass flow m/kg·s^{-1}	180
Isentropic efficiency η/%	90
Generation power N/MW	25
Rotating speed r/min	30,000

2 SCO2 TURBINE ROTOR DESIGN

In the design, a variety of rotational speed, flow diameter, blade stages, and turbine efficiency schemes were considered. According to results of the aerodynamic design a 4-stage turbine with a rotational speed of 30,000 r/min was finally determined. The design scheme is shown in **Figure 1**.

In addition, according to the actual demand, the generation power was set at 25 MW. The basic physical properties of CO_2 are listed in **Table 1**, and the design parameters of the turbine are listed in **Table 2**.

Based on the through-flow design, the preliminary design of the sCO_2 turbine rotor is completed. The layout is as follows: The turbine shafting adopts the form of a single-shaft double support, and the balance piston on the intake side is arranged opposite to the through-flow.

The gas flowing in the dry gas seal is discharged through the cooling sections at both ends, and the exhaust ports at both ends
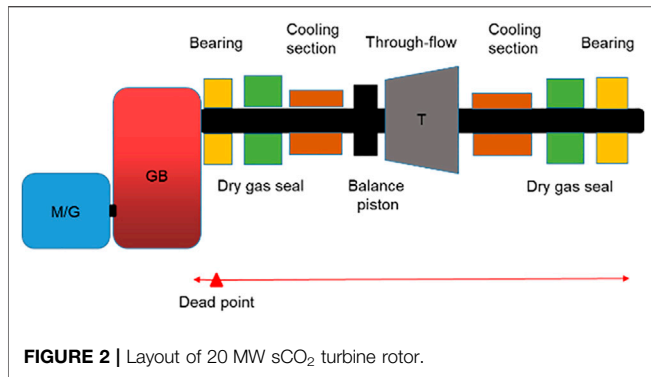
FIGURE 2 | Layout of 20 MW sCO$_2$ turbine rotor.

TABLE 3 | Rotor size of each part.

Shaft Position	Length(mm)	Diameter(mm)
Balance piston	480	260
Cooling section	220 × 2	180
Dry gas seal	200 × 2	180
Through flow + exhaust	480	192
Intake section	140	160
Length of shaft box	300 × 2	140

TABLE 4 | Key parameters of rotor.

Turbine rotor parameters	Value
Weight (kg)	850
Minimum shaft diameter (mm)	140
Maximum shaft diameter (mm)	260
Total span (mm)	2,540
Torsional stress (MPa)	44.5 (< 290)

are connected through the interlayer of the inner and outer cylinders. The intake side of the main gas is a thrust radial joint bearing, and the exhaust side is a supporting bearing. The bearing adopts tilting pad oil pressure sliding the bearing, and the rotor is connected to the transmission gearbox and the generator through a flexible coupling at the intake end. With the thrust bearing as the dead center, the rotor expands mainly to the right. The balance piston and the rotor are processed in the whole section, and the blades are installed in the circumferential direction. Since the shaft end needs to be arranged with dry gas seals and conventional dry gas seals have requirements on the temperature and pressure of the working environment, it is necessary to design a cooling gas for the shaft seal that reduces temperature and pressure. The system layout is shown in **Figure 2**.

The key parameters are calculated by setting the 3D model, and a preliminary torque check is carried out. The results are shown in **Table 4**.

According to the idea of the basic layout of the rotor, the size of the shaft section of the turbine rotor is preliminarily estimated, and the size design of the turbine rotor is completed for thermal

TABLE 5 | Materials of key components.

Components	Material
Rotor	GH 4169
Outer cylinder	ZG15Cr1Mo1 V
Inner cylinder	Alloy 625 cast
Blade	GH 4169
End seal body	Alloy 625 cast
Faceted bolts in inner cylinder	GH 4169
Faceted bolts in outer cylinder	20Cr1Mo1VNbTiB

TABLE 6 | Wall thickness summary comparison.

Minimum Wall Thickness of Inlet Volute/mm	50
Minimum wall Thickness of balance piston/mm	60
Minimum wall thickness of through-flow cylinder/mm	50
Minimum wall thickness of gas inlet/mm	50

stress analysis and expansion calculation. The calculation results are then provided back to the rotor designer to rerevise the rotor size and finally determine the size of each key part of the rotor. The detailed parameters are shown in **Table 4**.

Torsional Stress Check Formula

$$\tau = \frac{T}{W_p} = \frac{9.55 \times 10^{6\frac{P}{n}}}{0.2d^3} \le [\tau] \tag{1}$$

P- the power transmitted by the shaft, kW.

[τ]- the allowable torsional shear stress, MPa.

T-the torque received by the shaft, mm.

W- the torsional section coefficient of the shaft, mm^{3}N·

n-the rotational speed of the shaft, r/min

d-the diameter of the shaft at the calculated section, mm.

3 DESIGN OF THE SCO$_2$ TURBINE CYLINDER

3.1 Main Material

The main gas parameters are 24 MPa and 600°C, while the turbine speed reaches 30,000 r/min. The strength requirements are strict, so the rotor material is selected to be GH4169 as indicated in **Table 5**. To avoid t friction between the rotor and inner cylinder, the same type of nickel-based alloy material needs to be used to ensure consistent the linear expansion coefficient. The material selection scheme is shown in **Table 5**. The inner cylinder, rotor and blades are made of nickel-based materials, and the outer cylinder is made of ferrite material 9–12Cr steel. The selected materials are all mature materials that have been widely used in the field of ultra-supercritical steam turbines worldwide.

3.2 Inner and Outer Cylinder Design

The 25 MW sCO$_2$ turbine adopts a double-ground bearing support form, an efficient single-process reaction through-flow and a direct-connected tangential gas intake. To overcome the

difficulties of a high-density sCO$_2$ and large aerodynamic and centrifugal loads on the rotor blades, a 3D modeling of the T-shaped, pre-twisted rotor blades was completed. For the high-parameter, high-pressure inner cylinder, a shrink ring seal with low thermal stress constraints was developed. Key dimensions and parameters, such as interference, are determined through finite element analysis. Because of the high critical pressure of CO$_2$, dry gas seals at the ends are required, and a unique end gas seal and its cooling system are designed for this purpose. Flow-solid coupling calculations were selected to evaluate the influence on the temperature and stress field of the dynamic and static components. Finally, the main layout and structure plan of the preliminary design stage are planned.

The 3D design diagram of the turbine cylinder is drawn according to the rotor structure dimensions in **Table 3** and **Table 4** and the overall layout of the turbine in **Figures 1**, **2** (see **Figure 3**).

The turbine cylinder is designed with a double-layer cylinder structure, and the inner and outer cylinders are sealed with a horizontal mid-section and flange bolt seal. The thickness of the inner cylinder is 50 mm and that of the outer cylinder is 60 mm. The inner diameter of the intake port is 120 mm and that of the exhaust port is 260 mm. The inner cylinder is supported by the horizontal mid-section of the outer cylinder. The top and bottom are positioned and guided by positioning pins to ensure that the inner and outer cylinders can freely shrink and expand. The single-flow design is adopted, and the balanced piston gas seal is designed on the intake side to reduce the entire through-flow thrust. The stator blades of all stages are directly installed on the overall inner cylinder, and cooling flow is introduced at the gas seals at the ends of the outer cylinder on both sides to cool the shaft section, preventing the high-temperature failure of the dry gas seal.

The wall thickness is determined by **Eqs. 2**, **3**.

According to the thin-walled cylinder bearing stress formula:

$$\sigma = \frac{\Delta PD}{2\delta} \le [\sigma] \tag{2}$$

and we have:

$$\delta \ge \frac{\Delta PD}{2[\sigma]} \tag{3}$$

where:

σ—Stress.

△P—Pressure difference between the inside and outside cylinder walls.

D—Inner diameter of the pressure cylinder wall (without opening).

δ—Wall thickness of equal-walled cylinder.

According to the pressure difference between the inlet and the exhaust gas, it is estimated that the minimum wall thickness of the inlet volute is 50 mm, and the average stress is 40 MPa. To find the minimum wall thickness of the balance piston cylinder, the following discussion is used: According to the pressure difference between the inlet and exhaust gas of the first gear gas seal, as shown in **Table 6**, the minimum wall thickness is estimated to be
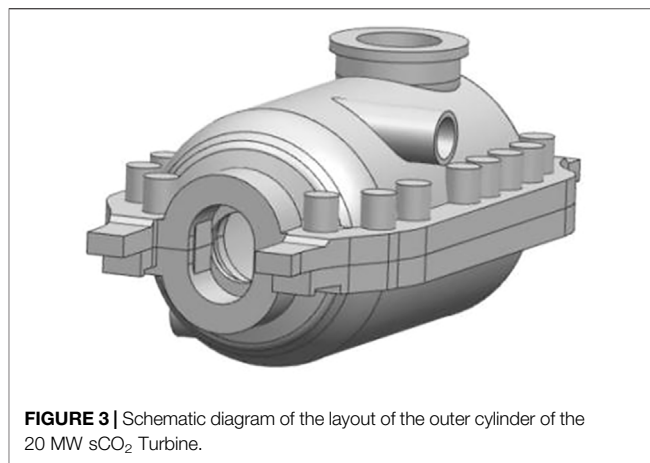

FIGURE 3 | Schematic diagram of the layout of the outer cylinder of the 20 MW sCO$_2$ Turbine.

60 mm, and the average stress is 20 MPa: According to the pressure difference between the inlet and exhaust gas of the first stage vane, the minimum wall thickness of the through-flow cylinder is estimated to be 50 mm, and the average stress is 26 MPa. The minimum wall thickness of the gas inlet should also be assessed according to the pressure difference there. Due to the small diameter, the design wall thickness can be very thin; however, considering that it would be matched with the cannula, the preliminary design should be considered as 50 mm.

The intake cylinder module of the turbine is supported on the front and rear bearing seats through cat claws, where the front cat claws simultaneously serve as the absolute center of the cylinder expansion, and the cylinder and the rotor expand in the same direction. The main control valve of the turbine is arranged on the left and right sides of the cylinder. The intake valve is directly connected to the outer cylinder through flanges and bolts. No gas guide pipe is required in the design. Laminated seals prevent leaks. The gas intake of the cylinder is adopted by the horizontal high and low tangential gas intake on both sides, the circulation part is implemented by the whole circumference gas intake, and the balance piston and the rotor are processed in the whole section. The cylinder exhaust is an upper exhaust port, which is connected to the exhaust pipe through a flange. The dry gas seal is designed so that the cylinder module is set on the outer cylinder, fixed by pins and expands at the same time as the outer cylinder. The influence of the expansion difference should be considered when designing the dry gas seal gap.

3.3 Analysis of Rotor Temperature Field

In the cooling gas design, when a large amount of cooling gas is used to lower the temperature of the rotating parts by forced convection cooling, it will cause greater thermal stress and thermal deformation, which will affect the safety of the components. However, when a small amount of gas is used, with the cooling scheme that isolates the outward tendency of the heat source, it can not only ensure the temperature limit of the contact surface between the shaft end and the dry gas seal but also, at most, limit the radial thermal stress gradient and thermal deformation. Therefore, when designing the cooling gas, it is necessary to fully ensure that the shaft end is not overheated and

FIGURE 4 | CHT Calculate the temperature distribution.

FIGURE 5 | Undamped critical speed of rotor.
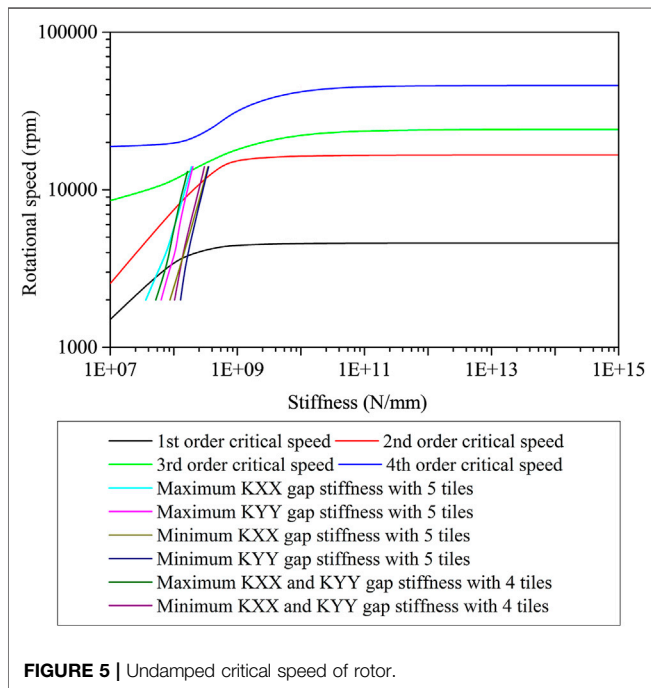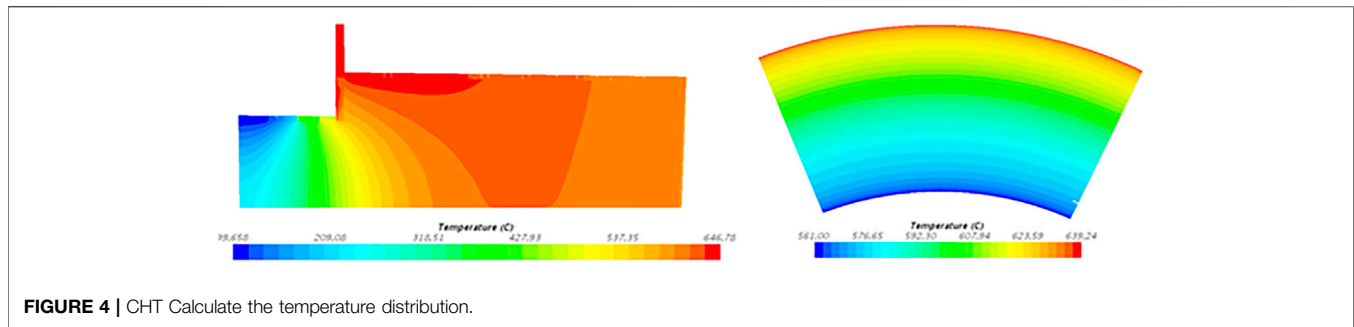
to control the temperature by inputting a cooling source; on the other hand, it is also necessary to reduce the thermal stress and thermal deformation on the surface of the rotor and to control the temperature difference by reducing the gas flow through the part's surface. After analyzing the temperature field, it is most suitable to use a 120°C cooling gas. The temperature field change at the end of the rotor is shown in **Figure 4**, and the maximum temperature reaches 646.76°C.

After the dynamic analysis of the shafting, its response peak-to-peak value, critical speed avoidance rate and Class I stability can all meet the requirements of API 684. The analysis of the undamped critical speed shows that the critical speed of the first-order rigid support of the rotor is 4,649 r/min, and the rotor operates as a flexible rotor. The undamped critical speeds are 3,924 r/min, 9,630 r/min, and 13,200 r/min, respectively, as shown in **Figure 5**. The first and second types of unbalanced responses are calculated for the rotor, and the damped critical speeds are 4,133 r/min and 16,200 r/min, respectively (according to API 684, 10867 r/min is not judged as a critical speed), and its avoidance rate satisfies the API 684 request. The damped

unbalanced response analysis shows that at the rated speed, the peak-to-peak response (maximum 7.7 μm) at the rotor front and rear axle inclinations meet the API 684 requirement of 25.4 μm. Under the condition of one time impeller cross-coupling stiffness, the logarithmic decay rate at the rated speed is greater than 0.1 regardless of whether it is supported by four-tiles or five-tiles bearings, and the rotor stability meets the requirements of API 684. The dynamic characteristics of the rotor supported by the 5-W and 4-W bearings are similar, and the logarithmic decay rate is larger while the stability is better at the rated speed of the 4-W bearing.
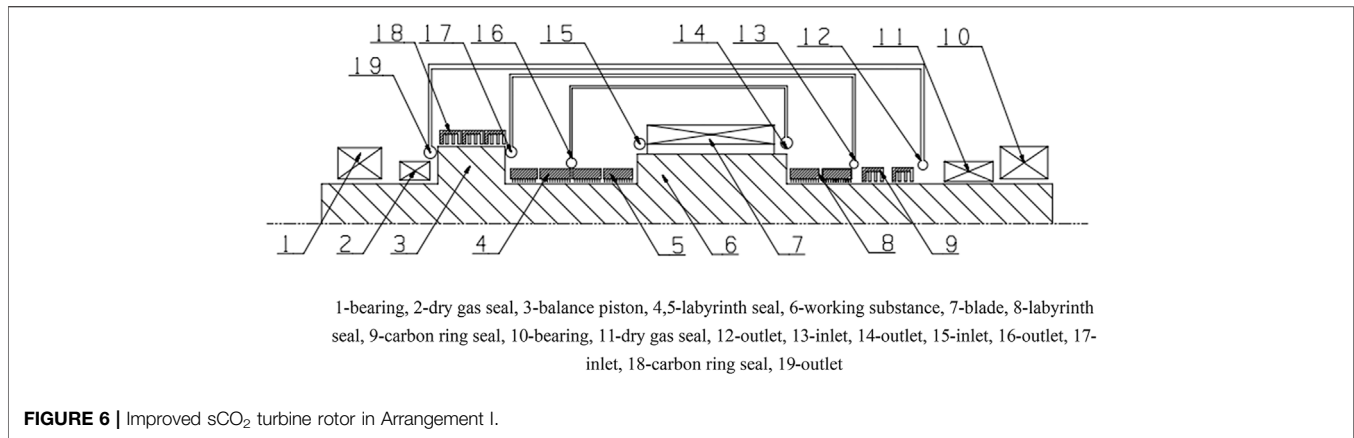
4 OPTIMIZATION OF SCO$_2$ TURBINE ARRANGEMENT

This design results in a large amount of leakage due to the large balance between piston length and diameter. The increase in the overall arrangement length of the rotor will lead to many problems in the structural design of the sCO$_2$ turbine rotor, such as endurance strength checks and creep stress assessments. Therefore, two schemes to optimize the arrangement of sCO$_2$ turbines are proposed.
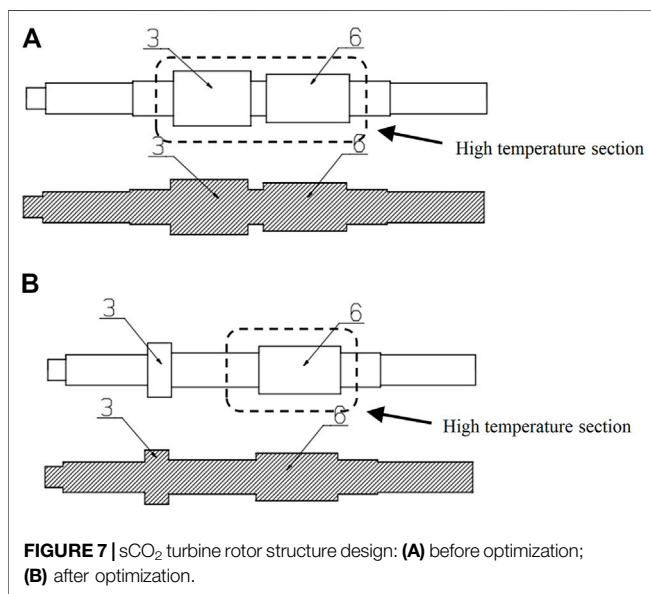
4.1 Optimization Scheme I

To ensure that the shaft seal is cooled, with the exhaust pressure and balance thrust at the shaft end being reduced, the length of the balance piston being reduced, and the leakage of the high-temperature medium being reduced, which is conducive to the operation of the dry gas seal, the rotor structure and system of the turbine is optimized to balance the axial force, and the arrangement of the turbine rotor balance piston and the cooling position of the cooling gas are changed, shown in **Figure 6**.

The balance piston is arranged in the cooling gas section. Due to the low temperature of the turbine cooling gas section, the carbon ring seal can be arranged. Compared with the clearance of 0.5 mm of the ordinary seal, the carbon ring seal can achieve a clearance of 0.1 mm. However, the carbon ring seal has certain requirements for the ambient temperature and cannot be arranged in the high-temperature area. This arrangement can greatly reduce the length of the balance piston and the length of the high-temperature section of the rotor during turbine operation, which can decreases the thermal stress, thus
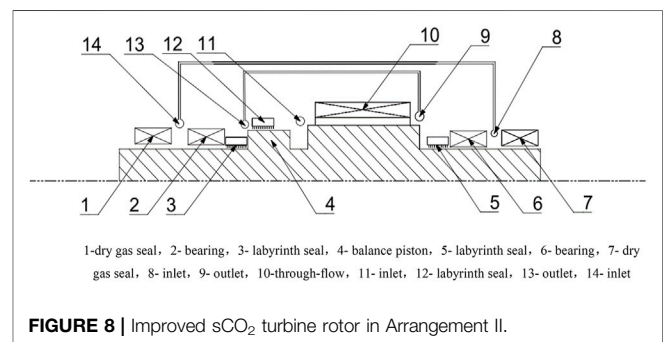
1-bearing, 2-dry gas seal, 3-balance piston, 4,5-labyrinth seal, 6-working substance, 7-blade, 8-labyrinth seal, 9-carbon ring seal, 10-bearing, 11-dry gas seal, 12-outlet, 13-inlet, 14-outlet, 15-inlet, 16-outlet, 17-inlet, 18-carbon ring seal, 19-outlet

FIGURE 6 | Improved sCO$_2$ turbine rotor in Arrangement I.

FIGURE 7 | sCO$_2$ turbine rotor structure design: (A) before optimization; (B) after optimization.

1-dry gas seal, 2- bearing, 3- labyrinth seal, 4- balance piston, 5- labyrinth seal, 6- bearing, 7- dry gas seal, 8- inlet, 9- outlet, 10-through-flow, 11- inlet, 12- labyrinth seal, 13- outlet, 14- inlet

FIGURE 8 | Improved sCO$_2$ turbine rotor in Arrangement II.

improves the safety performance of the unit and reduces the leakage of mainstream gas to improve the operation efficiency. The leakage of mainstream gas is reduced by 0.5%. The inlet and exhaust of the cooling gas are independent, and the gas source is stable. The inlet and exhaust pressures of the cooling gas can be adjusted according to the requirements. The balance piston is used to balance the axial thrust of the flow passage of the rotor and sealing teeth. In this design, the size and length of the balance piston can be adjusted by modifying the inlet and exhaust pressure of the cooling gas, which can effectively control the size of the balance piston.

The arrangement of the cooling gas system enables the pressure to be reduced to a controllable pressure, which is the allowable design value of the dry gas seal. By applying cooling and pressure reduction designs in the system arrangement, the dry gas seal can operate normally, and the thermal stress of the rotor can be reduced by adjusting the temperature of the cooling gas.

The improvement of the turbine rotor arrangement and system can greatly shorten the overall span of the rotor. As

shown in **Figure 7**, by improving the arrangement of the rotor, the length of the high-temperature section is reduced from 1,100 mm to 750 mm, which is a reduction of 32%; the length of the balance piston is reduced from 480 mm to 220 mm, which is a reduction of 54%; and the overall length of the rotor is reduced from 2,540 mm to 2,310 mm, which is a reduction of 9%.

4.2 Optimization Scheme II
This scheme is conducive to the overall structural design of the rotor, improves the safety performance of the rotor and can appropriately reduce the shaft diameter to improve the economic performance of the turbine unit.

The oil bearing is arranged outside the dry gas seal in the previous scheme, so the isolation gas needs to be set to prevent the oil gas of the oil bearing from entering the dry gas seal. The dry gas seal must be disassembled horizontally in the primary scheme. The disassembly of the dry gas seal is more troublesome if the oil bearing is arranged outside. In addition, a separate cooling system should be designed for the cooling gas in the shaft seal cooling section; otherwise, the excessive temperature could lead to the leakage of the working medium in the inner cylinder. These factors lead to the complexity of the arrangement of the rotor system and the large span of the rotor, which is not conducive to rotor dynamics design, safety verification and turbine operation.

A scheme is proposed in which the gas bearing replaces the oil bearing and combines with the cooling section to improve the

1-rotor 2-gas bearing 3-outer cylinder 4-dry gas seal

FIGURE 9 | sCO$_2$ turbine gas bearing arrangement diagram.
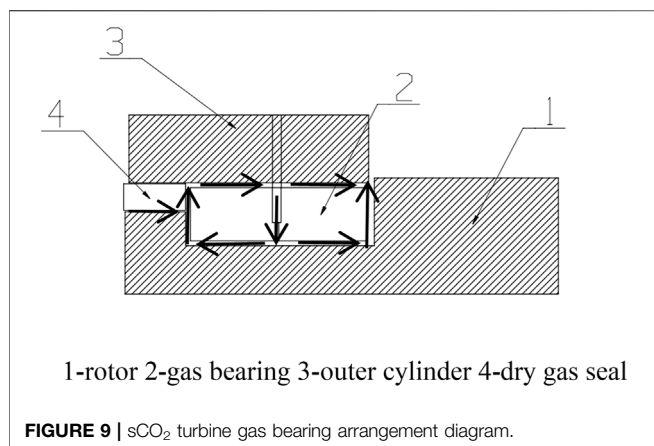
previously discussed shortcomings, as shown in **Figure 8**. The dry gas seals at both ends of the turbine are installed outside the gas bearing, which is combined with the original cooling section. This design has three advantages. First, by arranging the gas bearing inside the dry gas seal, the gas from the gas bearing can play the role of cooling gas at the same time, so a separate cooling section does not need to be arranged. The rotor and outer cylinder are cooled by the flow of the gas bearing, which can greatly reduce the overall length of the shaft, compact the overall structure and greatly improve the safety of the system. Second, the cooling gas system does not need to be designed separately, and no lubricating oil system is needed, so the isolation gas to prevent the oil gas from leaking into the dry gas seal is not needed. This design effectively reduces the complexity of the system. In addition, the arrangement of gas bearings can improve the service life of the bearing components of the turbine unit, reduce the mechanical loss of turbine rotation and improve the turbine efficiency. The flow direction design and specific structure of the cooling gas are shown in **Figure 9**.

By improving the rotor arrangement and system, compared to the original design, the length of the balance piston remains unchanged from the original 480 mm, and the length of the high-temperature section remains 1,100 mm. However, the mechanical loss is reduced by 0.3%. In this scheme, no additional cooling system is needed, so 440 mm of the cooling section is reduced to 0 mm, and the overall rotor length is reduced from 2,540 mm to 2,100 mm, which is a reduction of approximately 17%. This is conducive to rotor structural design and reduces the mechanical loss of rotor rotation.

In consideration of the requirements of gas bearings for rotor speed, weight and load, Scheme II is more suitable for sCO$_2$ turbine

rotor arrangements with high speed (speed >3,000 r/min), low weight (weight less than 300 kg) and low load (load <10 MW).

5 CONCLUSION

In summary, to achieve a sCO$_2$ cycle power generation system, a 25 MW sCO$_2$ turbine rotor and cylinder were designed. In addition, two optimized design schemes of a sCO$_2$ turbine rotor were proposed. Finally, the advantages of the compact arrangement were analyzed by comparison with the traditional scheme. The main conclusions from this study are presented as follows:

(1) The improvement of turbine rotor arrangement can greatly shorten the overall span of the rotor. In Scheme I, the length of the high-temperature section is reduced by 32%, from 1,100 mm to 750 mm, and the length of the rotor is reduced by 9%, from 2,540 mm to 2,310 mm. In Scheme II, the length of the rotor is reduced by 17%, from 2,540 mm to 2,100 mm.
(2) The compact arrangement increases the efficiency of the turbine. The gas leakage loss of the system is reduced by 0.5% in Scheme I, and the mechanical loss is reduced by 0.3% in Scheme II.
(3) Compared with the traditional turbine scheme, the length of the balance piston is reduced in the schemes proposed in this paper, which is more conducive to the arrangement and operation of dry gas seals.
(4) Considering the requirements of gas bearings for rotor speed, weight and load, the arrangement in Scheme II is more suitable for the arrangement of sCO$_2$ turbine rotors with low load and low weight.

DATA AVAILABILITY STATEMENT

The raw data supporting the conclusion of this article will be made available by the authors, without undue reservation.

AUTHOR CONTRIBUTIONS

CL and JS contributed to conception and design of the study. ZL, WB, LJ and NH conducted the investigation and wrote the first draft of the manuscript. All authors contributed to manuscript revision, read, and approved the submitted version.

REFERENCES

Ahn, Y., Bae, S. J., Kim, M., Cho, S. K., Baik, S., Lee, J. I., et al. (2015). Review of Supercritical CO2 Power Cycle Technology and Current Status of Research and Development. *Nucl. Eng. Technol.* 47 (6), 647–661. doi:10.1016/j.net.2015.06.009

Crespi, F., Gavagnin, G., Sánchez, D., and Martínez, G. S. (2017). Supercritical Carbon Dioxide Cycles for Power Generation: A Review. *Appl. energy* 195, 152–183. doi:10.1016/j.apenergy.2017.02.048

Du, Y., Tian, G., and Pekris, M. (2022). A Comprehensive Review of Micro-scale Expanders for Carbon Dioxide Related Power and Refrigeration Cycles. *Appl. Therm. Eng.* 201, 117722. doi:10.1016/j.applthermaleng.2021.117722

Guo, J.-Q., Li, M.-J., He, Y.-L., Jiang, T., Ma, T., Xu, J.-L., et al. (2022). A Systematic Review of Supercritical Carbon dioxide(S-CO2) Power Cycle for Energy Industries: Technologies, Key Issues, and Potential Prospects. *Energy Convers. Manag.* 258, 115437. doi:10.1016/j.enconman.2022.115437

Kalra, C., Hofer, D., Sevincer, E., Moore, J., and Brun, K. (2014). "Development of High Efficiency Hot Gas Turbo-Expander for Optimized CSP Supercritical CO2 Power Block Operation," in *The Fourth International Symposium—Supercritical CO2 Power Cycles (sCO2): Citeseer* (Southwest Research Institute), 1–11.

Khanmohammadi, S., Kizilkan, O., and Ahmed, F. W. (2020). Tri-objective Optimization of a Hybrid Solar-Assisted Power-Refrigeration System Working with Supercritical Carbon Dioxide. *Renew. Energy* 156, 1348–1360. doi:10.1016/j.renene.2019.11.155

Kim, T. W., Jeong, W. S., and Suh, K. Y. (2008). Numerical Modeling and Analysis of Supercritical Carbon Dioxide Turbine. *Trans. Am. Nucl. Soc.* 98 (1), 449–450. doi:10.1016/j.nucengdes.2015.08.016

Kim, T. W., Kim, N. H., and Suh, K. Y. (2006). Computational Fluid Dynamics Analysis for an Optimal Supercritical Carbon Dioxide Turbine Blade. *Trans. Am. Nucl. Soc.* 95, 790–791. doi:10.1115/ICONE16-48240

Lee, J., Lee, J. I., Ahn, Y., and Yoon, H. (2012). "Design Methodology of Supercritical CO2 Brayton Cycle Turbomachineries," in Turbo Expo: Power for Land, Sea, and Air, June 11–15, 2012 (Copenhagen, Denmark: American Society of Mechanical Engineers (ASME)), 975–983. doi:10.1115/GT2012-68933

Li, Z., Liu, X., Shao, Y., and Zhong, W. (2020). Research and Development of Supercritical Carbon Dioxide Coal-Fired Power Systems. *J. Therm. Sci.* 29 (3), 546–575. doi:10.1007/s11630-020-1282-6

Liao, G., Liu, L., E, J., Zhang, F., Chen, J., Deng, Y., et al. (2019). Effects of Technical Progress on Performance and Application of Supercritical Carbon Dioxide Power Cycle: A Review. *Energy Convers. Manag.* 199, 111986. doi:10.1016/j.enconman.2019.111986

Luo, D., Liu, Y., Sun, X., and Huang, D. (2017). The Design and Analysis of Supercritical Carbon Dioxide Centrifugal Turbine. *Appl. Therm. Eng.* 127, 527–535. doi:10.1016/j.applthermaleng.2017.08.039

Marion, J., Kutin, M., McClung, A., Mortzheim, J., and Ames, R. (2019). "The STEP 10 MWe sCO2 Pilot Plant Demonstration," in Turbo Expo: Power for Land, Sea, and Air, June 17–21, 2019 (Phoenix, Arizona, USA: American Society of Mechanical Engineers (ASME)). doi:10.1115/GT2019-91917

Mohammed, R. H., Alsagri, A. S., and Wang, X. (2020). Performance Improvement of Supercritical Carbon Dioxide Power Cycles through its Integration with Bottoming Heat Recovery Cycles and Advanced Heat Exchanger Design: a Review. *Int. J. Energy Res.* 44 (9), 7108–7135. doi:10.1002/er.5319

Odabaee, M., Sauret, E., and Hooman, K. (2016). CFD Simulation of a Supercritical Carbon Dioxide Radial-Inflow Turbine, Comparing the Results of Using Real Gas Equation of Estate and Real Gas Property File. *Appl. Mech. Mater.* 846, 85–90. doi:10.4028/www.scientific.net/AMM.846.85

Qi, H., Gui, N., Yang, X., Tu, J., and Jiang, S. (2018). The Application of Supercritical CO2 in Nuclear Engineering: A Review. *J. Comput. Multiph. Flows* 10 (4), 149–158. doi:10.1177/1757482x18765377

Schmitt, J., Willis, R., Amos, D., Kapat, J., and Custer, C. (2014). "Study of a Supercritical Co2 Turbine with Tit of 1350 K for Brayton Cycle with 100 Mw Class Output: Aerodynamic Analysis of Stage 1 Vane," in Turbo Expo: Power for Land, Sea, and Air, June 16–20, 2014 (Düsseldorf, Germany: American Society of Mechanical Engineers (ASME)). doi:10.1115/GT2014-27214

Shi, D., Li, L., Zhang, Y., and Xie, Y. (2015). "Thermodynamic Design and Aerodynamic Analysis of Supercritical Carbon Dioxide Turbine," in Proceedings of the 2015 International Conference on Electromechanical Control Technology and Transportation (Zhuhai, China): Advances in Engineering Research). doi:10.2991/icectt-15.2015.9

Wang, Y.Q., Shi, D. B., Zhang, D., and Xie, Y. H. (2016). Study on Aerodynamic Performance of a Partial-Admission Supercritical Carbon Dioxide Radial-Inflow Turbine. *Therm. Turbine* 45, 184–195.

Wu, C., Xu, X., Li, Q., Li, J., Wang, S., and Liu, C. (2020a). Proposal and Assessment of a Combined Cooling and Power System Based on the Regenerative Supercritical Carbon Dioxide Brayton Cycle Integrated with an Absorption Refrigeration Cycle for Engine Waste Heat Recovery. *Energy Convers. Manag.* 207, 112527. doi:10.1016/j.enconman.2020.112527

Wu, P., Ma, Y., Gao, C., Liu, W., Shan, J., Huang, Y., et al. (2020b). A Review of Research and Development of Supercritical Carbon Dioxide Brayton Cycle Technology in Nuclear Engineering Applications. *Nucl. Eng. Des.* 368, 110767. doi:10.1016/j.nucengdes.2020.110767

Yu, A., Su, W., Lin, X., Zhou, N., and Zhao, L. (2020). Thermodynamic Analysis on the Combination of Supercritical Carbon Dioxide Power Cycle and Transcritical Carbon Dioxide Refrigeration Cycle for the Waste Heat Recovery of Shipboard. *Energy Convers. Manag.* 221, 113214. doi:10.1016/j.enconman.2020.113214

Zhang, H., Zhao, H., Deng, Q., and Feng, Z. (2015). "Aerothermodynamic Design and Numerical Investigation of Supercritical Carbon Dioxide Turbine" in Turbo Expo: Power for Land, Sea, and Air, June 15–19, 2015 (Montreal, Quebec, Canada: American Society of Mechanical Engineers (ASME)). doi:10.1115/GT2015-42619